International Journal of Agriculture, Environment and Food Sciences
e-ISSN : 2618-5946
www.jaefs.com
JAEFS
edit PUBLISHING

Research Article
Int J Agric Environ Food Sci 6 (1): 108-120 (2022)

Application of swat hydrological model to assess the impacts of land use change on sediment loads

Rouhollah Nasirzadehdizaji **Dilek Eren Akyuz***

Istanbul University - Cerrahpasa, Department of Civil Engineering, 34320 Avcılar, Istanbul, Türkiye

*Corresponding Author: dilekeren.akyuz@iuc.edu.tr

Citation
Nasirzadehdizaji, R. and Akyuz, D.E. (2022). Application of swat hydrological model to assess the impacts of land use change on sediment loads. Journal of Agriculture, Environment and Food Sciences, 6 (1), 108-120.
Doi
https://doi.org/10.31015/jaefs.2022.1.15

Received: 02 January 2022
Accepted: 06 March 2022
Published Online: 24 March 2022
Revised: 02 April 2022

Year: 2022
Volume: 6
Issue: 1 (March)
Pages: 108-120

Available online
http://www.jaefs.com
https://dergipark.org.tr/jaefs

Abstract

Controlling and reducing the watershed's erosion and sedimentation is essential to ensure the continuity of projects implemented to develop land and water resources and improve sustainability, performance, and longevity. Sediment control is also critical in managing the river basin in limiting the transport of solids, improving water quality, sustaining aquatic life, and preventing damage to downstream aquatic environments and ecosystems. Estimating the potential effects of land-use changes on surface runoff and soil erosion requires distributed hydrological modeling methods. In addition to naturally occurring sediments, changes in land-use types for different applications can be a primary cause for the increase in sediment rates in the watershed. This study used the Soil and Water Assessment Tool (SWAT), a rainfall-runoff model, to evaluate land use/cover changes (i.e., deforestation) and their impact on sediment load under different scenarios. For the baseline (no changes) scenario, the watershed is calibrated using the flow and sediment data measured from the rain gauge station during the time step to estimate the post-deforestation changes at the sub-catchment scale of the study area. The study results indicated that the total surface runoff and sediment yield for the selected sub-catchment in the deforestation scenario with the highest spatial distribution, due to the high erosivity (24% increase) of excessive surface runoff after deforestation, sediment yield increased 3.5-fold. In contrast, due to the removal of trees and vegetation's canopy, the evapotranspiration, leaf area index, and dissolved oxygen transported into reach showed the inverse ratios, and the values decreased by 5%, 24, and 17%, respectively, in compared with the baseline scenario. In terms of watershed management, therefore, the application of hydrological models such as SWAT rainfall-runoff and erosion models can be a helpful method for decision-makers to apply for the protection of forests from intensive impacts such as deforestation and limiting their socio-environmental effects.

Keywords

Rainfall-runoff model, Deforestation, Agriculture, Soil erosion, Watershed management, Göksu-Çanakdere

Introduction

Erosion and sedimentation issues and their impact on water resources and the environment are unavoidable and remain significant challenges for watershed management with high soil erosion rates. Erosion processes remove rock or soil and lead to the formation of mineral sediment. The sediment moves with water (surface runoff), wind, or ice, and deposits in new locations by gravity acting on the particles. Water's kinetic energy causes the wash of sediments down from the surface into a stream and eventually to the river's delta. There are complex interactions on the scale of river sections and basins, which affect the movement of sediments and the generation of habitat types in the river (Bettess et al., 2011; Gellis et al., 2016). Sediment can accumulate under, in, or around structures such as bridges, conduits, reservoirs, and water intakes. This process leads to cracks in the riverbed, severe stream instability, and eventually unusual flow around engineering structures such as bridge piers or culverts. Unlike frequent low-flow flood events, rare high-flow flood events can transport more sediment, leading to

sudden sediment accumulation. Different phenomena such as ground deformations or landslides can also lead to the overrun of sediments in the river system and form an unexpected build-up of sediments deposition.

In addition to the naturally-occurring sediment, it may also originate from human practices on the land. The impact of agriculture, deforestation, mining, urbanization, and road building on soil erosion rates is inevitable (Amundson et al., 2015; Hassan et al., 2017). In agricultural activities, soil erosion occurs through the field's topsoil wearing away off by the natural physical or chemical forces of water and wind or through forces incorporated with the farming activities such as plowing and tillage (Ritter, 2012). The world's rapid population growth leads the urbanization and changing land-use. On the other hand, population growth leads to increased food demand in many countries. Hence the agricultural sector is being put under excessive pressure to produce and provide enough food for the growing communities. With soil erosion, the most productive and valuable soil profile used for agricultural purposes will be lost through the reduced capacity of the soil for storing water and nutrients with the poor physical and chemical properties of the subsoil (Langdale et al., 1992). Degraded land is also often unable to retain water, exacerbating flooding. The impact of soil erosion is not just the loss of fertile land. It leads to increased water pollution and reduces dissolved oxygen, reducing fish and other species. Therefore, the loss of productive topsoil with rich organic matter lowers the crop yield potential due to the degraded soil structure and the reduction of nutrients that were contained in the organic matter (Brevik, 2006; Wardle et al., 2004), increased production costs (Pimentel and Burgess, 2013), and thus will cause the increased demand for agricultural commodities.

Consequently, the above reasons will create an impetus to convert forests and grasslands into farmland (Izquierdo and Grau, 2009). Forests have a variety of ecological and hydrological benefits, for example, contributing to enhanced infiltration and water retention. Therefore, filtration in the soil column helps to improve water quality (Bredemeier, 2010). Furthermore, the combining effects of vegetation, litter cover, and less water yield imply lower erosion rates under forest cover, primitive sedimentation, mitigating flood hazards, and affecting both the soil quality and the downriver aquatic environments (Farley et al., 2005; Owens et al., 2005; Schüler, 2006).

Degradation of forests for agriculture and timber leads to a significant increase in soil erosion rates by losing forest-derived leaf litter and plant roots. The role of the leaf litter is to protect the soil below from wind and water erosion and protect the plant roots that hold soil particles to and below the soil surface. (Avwunudiogba and Hudson 2014; Pimentel et al., 1995; Wenger et al., 2018). In addition to logging, forest fires have been the most common method of destroying forests. Forest fires either have a natural origin or are caused by human activities. Depending on the situation, natural wildfires are caused mainly by lightning, volcanoes, meteors, and coal seam fires. However, on a global scale, only about 4% of forest fires are caused by natural causes; in all other cases, humans are responsible for fires-whether directly or indirectly, intentionally or due to negligence (WWF, 2017). The anthropic causes of fires are agriculture displaying and ranching, which are constitute the highest level of association with forest fires (Juárez-Orozco et al., 2017).

Forest degradation by converting forest lands to dry farming and deforestation-induced impacts soil redistribution. In addition, these activities can lead to species loss and degradation of ecosystem functions, consequently affecting terrestrial ecosystems (Maxwell et al., 2016; Rocha-Santos et al., 2016). Therefore, through the changes in hydrological processes, degradation of forests for agriculture cause clear impacts to the freshwater in the downstream and estuarine environments with an increase in the amount of sediment (Iwata et al., 2003; Jenkins et al., 2007; Pattanayak and Wendland, 2007).

Predicting the potential effects of land-use changes, for example, deforestation and degradation of forests for agriculture on runoff and soil erosion, require the development of distributed hydrological modeling methods. The ecological, biological, climatological, biodiversity, socio-economic, and hydrological impacts of the deforestation and degradation of the forests have been investigated throughout various studies (Aliye et al., 2014; Bonan, 1999; Chrisphine et al., 2015; Hughes et al., 2000; Li et al., 2016; Symes et al. 2018; Wilk et al., 2001). Conversely, the potential of applications of the hydrologic and numerical models have not been thoroughly investigated to improve the conception of deforestation impacts on runoff and erosion-sedimentation and to plan relevant mitigation strategies by managers against the negative consequences of degradation of the forest,

This study investigates the potential of applying the SWAT hydrological model to examine the impact of degradation of forests for agriculture on sediment load. The purpose of this study is to evaluate the hydrological consequences of possible deforestations and their effects on streamflow and use runoff and erosion models to analyze their respective impacts on sediment load.

Materials and Methods

In the context of this work, we investigated the effect of land-use changes, namely the degradation of forests for agricultural activities, on surface runoff and sediment yield at the sub-basin scale. To this end, we designed land-use change (deforestation) scenarios. To predict the hydrological response to the changes, we applied the rainfall-runoff model using the meteorological and basin characteristic data (land-use, soil, and topography). The model is calibrated using observed flow and suspended sediment concentration data. In terms of management practices, the findings in this study can be used in dealing with hydrological risks and environmental issues in the Göksu-Çanakdere rivers' watershed.

Site description

The Göksu-Çanakdere rivers' watershed (40° 59” N, 29° 51” E), with an area of approximately 800 km^2, is in north-east of Istanbul and west of Kocaeli province, Turkey, reaching into the Black Sea (Figure 1). Its climate is characterized by the Black Sea region, the Balkans, and Anatolia. The two main tributaries in the study area are Göksu and Çanakdere, with a total length

of 122 and 77 km, respectively. The geological types include clay-limestone, sandy limestone, sandstone, and limestone (Citiroglu et al., 2011). The topographic pattern is partly undulating, ranging from 1 to 649 m elevation. The annual temperatures range from 8°C to 15°C, and annual rainfall ranges from 350 to 1400 mm (Aksoy et al., 2010). The average annual rainfall in the basin is about 815 mm, and the average annual temperature is about 14.8 °C. (State Meteorological Service (MGM). Flow and suspended sediment data were purchased from the Turkish State of Hydraulics (DSI), which was collected from rain gauge stations located in major rivers. Göksu-D02A004 (41° 04' 40" N, 29° 46' 34" E), and Çanakdere-D02A149 (41° 04' 19" N, 29° 51' 08" E) are two rainfall stations used to measure flow and sediment data. The total rainfall catchment area for collecting data from these two stations is 782 square kilometers. The predominant land-use type in the watershed is agriculture (55.2%) and forest (43.6%). The largest forest area is in the central part of the watershed between Istanbul and Kocaeli Province, mainly covering Pure Oak Stands forests, with the rest being Mixed Stands Forest species (Atalay, 1986).

Land-use change scenario

Forests after agricultural lands are the most extensive in the region. Since most of the watershed is dedicated to agricultural activities and the fast-growing need for agricultural products to provide food resources, thus deforestation and conversion of forests into agricultural land is possible in the study area. Forest fires have always been the most common method of destroying forests and turning forests into farmland. Inland management agricultural activities play an important role in erosion control, agricultural pollutants, and water quality. Changes in land-use for agricultural purposes will also affect the hydrological response of the watershed. To study the impact of deforestation (i.e., after different forest fire scenarios) on the watershed, such as surface runoff, erosion, and sediment load, we designed baseline (pre-deforestation) and post-deforestation scenarios. This study was performed in two phases. The first phase corresponds to the baseline scenario. The model is calibrated and verified based on current land-use and meteorological data that have not changed from 2005 to 2017. The relevant rainfall event characteristics and model parameters did not change for the first scenario. In the second phase of the study, the forest patches which are destroyed due to the forest fires (forest fire scenarios) and converted to the non-irrigated arable land are defined for use in the model to analyze the effects of land-use change and its impacts on flow rates and sediment fluxes. In the proposed scenarios, homogeneous forest patches with 25%, 50%, and 100% burnt forest areas are defined for use in the model (Table 1). In this step, the land-use map is modified and used as a model input in the post-deforestation scenarios.

SWAT Model

Hydrological modeling involves simulating the conversion process of precipitation to runoff. In general, the hydrological model has two main components. In the first component, precipitation contributes to the formation of the hydrograph, while in the second component, the water flow distribution is used to determine the hydrograph profile. Therefore, the rainfall-runoff process can include rainfall simulation in the basin, infiltration and rainwater loss, and finally, the trend and movement of excess water in the area. In contrast, the first three processes are related to the first component and the last process attributed to the second component of the hydrologic model. This study has applied the SWAT model, a physical-conceptual model, to simulate the hydrological conditions and sediment response for the current watershed situation and different forest fire scenarios. The SWAT hydrological model is a semi-distributed model functioning on daily or sub-daily time steps and process-based, time-continuous simulation. It can be implemented for different management conditions over extended periods in small to large complex watersheds divided into hydrological response units (HRUs) based on dem, soil, and land-use types. The model developed to estimate the impacts of different management methods on hydrological and water quality processes, sediment yield, and pollution loads (Arnold et al., 1993; Yen et al., 2014) and is also used to analyze the effects of climate, soil, vegetation and agricultural activities on the discharge and chemical yields in watersheds. SWAT is being applied to model streamflow, sediment, and nutrient transport within a watershed (Neitsch et al., 2011) and find a good action plan, which depends mainly on the integrated watershed model (Collins and McGonigle, 2008; De et al., 2013). This model anticipates the effects of land management practices or climate change on sediment transport and hydrological response at the surface over the water catchments with different soils, land uses, and management practices (Neitsch et al., 2005).

Model set-up

In the SWAT model, the watershed is subdivided into multiple micro-basins, and each micro-basin is further subdivided into homogeneous parts named hydrological response units (HRUs). Each HRU is a homogeneous combination of land-use, management, topographical, and soil characteristics in each sub-basin (Arnold et al., 2012) to calculate water balance. Water balance in each HRU is an essential issue behind all processes in SWAT, as it affects plant growth, sediments movement, nutrients, pesticides, and pathogens. Water balance (Equation 1) is a function of inputs driven by climate parameters such as rainfall, temperature (maximum and minimum), solar radiation, wind speed, and relative humidity. The hydrological processes simulated by SWAT are including of surface runoff, evapotranspiration, lateral flow, infiltration, canopy storage, percolation, groundwater flow, tile drainage, water redistribution in the soil profile, return flow and recharge by infiltration from surface waters, ponds, and tributaries.

$$SW_t = SW_0 + \sum_{i=1}^{t}\left(R_{day} - Q_{surf} - E_a - w_{seep} - Q_{gw}\right) \quad (1)$$

where, the final soil water content, SW_t(mm H_2O) at the simulation time t (days), is obtained from the sum of SW_0 (mm H_2O), the initial soil water content on day i, and the amount of total precipitation, R_{day} (mm H_2O) on day i, when the total losses on day i including the amount of surface runoff, Q_{surf}(mm H_2O), the amount of evapotranspiration, E_a(mm H_2O), the amount of water that percolates from the soil profile, w_{seep}(mm

H_2O), and the amount of return flow Q_{gw}(mm H_2O), are subtracted from the total precipitation. SWAT uses the SCS curve number procedure (USDA, 1972) and the Green and Ampt (Green and Ampt, 1911) infiltration method to predict surface runoff. Penman-Monteith (Monteith, 1965), Hargreaves (Hargreaves and Samani, 1985), and Priestley-Taylor (Priestley and Taylor, 1972) are three methods recommended by the model to estimate potential evapotranspiration (PET). In order to predict the erosion of each HRU and the sediment yield of the sub-basin, the SWAT model uses the Modified Universal Soil Loss Equation (MUSLE) (Williams, 1975), as shown in Equation 2.

$$Sed = 11.8 * \left(Q_{surf} * q_{peak} * area_{hru}\right)^{0.56} * K_{USLE} * C_{USLE} * P_{USLE} * LS_{USLE} * CFRG \quad (2)$$

In which, Sed is the sediment yield to the stream network at the outlet on a given day (metric tons), Q_{surf} is the surface runoff volume from a given rainfall event (mm ha^{-1}), q_{peak} is the peak flow rate in $m^3 s^{-1}$, $area_{hru}$ is the area of the HRU (ha), K_{USLE} is soil erodibility factor (0.013 metric ton m^2 h-/(m^3 – metric ton cm)) which is a soil property available from the Universal Soil Loss Equation (USLE), C_{USLE} is the USLE cover (crop/vegetation) management factor and can be derived from land cover data, P_{USLE} is the USLE support conservation practice factor, the erosion baseline practice factor, which is a field-specific value, LS_{USLE} is the USLE topographic (slope length-gradient) factor, and $CFRG$ is the coarse fragment factor.

SWAT requires different input data to represent water and sediment yield spatial variability. The required input data are soil and land use/cover feature maps, topographic maps (Digital Elevation Model (DEM)), and climate data. The watershed's land-use/cover types are mainly agricultural and forest land. The CORINE Land Cover (CLC, 2018) dataset of the EU Copernicus Land Monitoring Service is used as land use/cover data to generate hydrological response units (HRU) for each sub-basin area. A significant land use/land cover is divided into 16 land-use categories, converted from the original land-use category to the appropriate SWAT land-use classification code, and defined using a lookup table, as shown in Table 2. The soil characteristic data was obtained from the Turkish soil dataset prepared by an interdisciplinary team composed of soil scientists, geologists, geomorphologists, and GIS experts (Cullu et al., 2018). The main soil types were reclassified according to the soil texture and hydrological soil groups (FAO soil classification), provided by the European Commission and the European Soil Bureau Network (Kük and Burgess, 2010). The meteorological data is obtained from the MGM (State Meteorological Service) for thirteen hydrological years (2005 to 2017) and simulated the SWAT model. The measured flow and sediment data collected from the Göksu and Çanakdere rain gauge stations are used for model calibration and verification. The main steps of the input and fitting process of the SWAT model are shown in Figure 2.

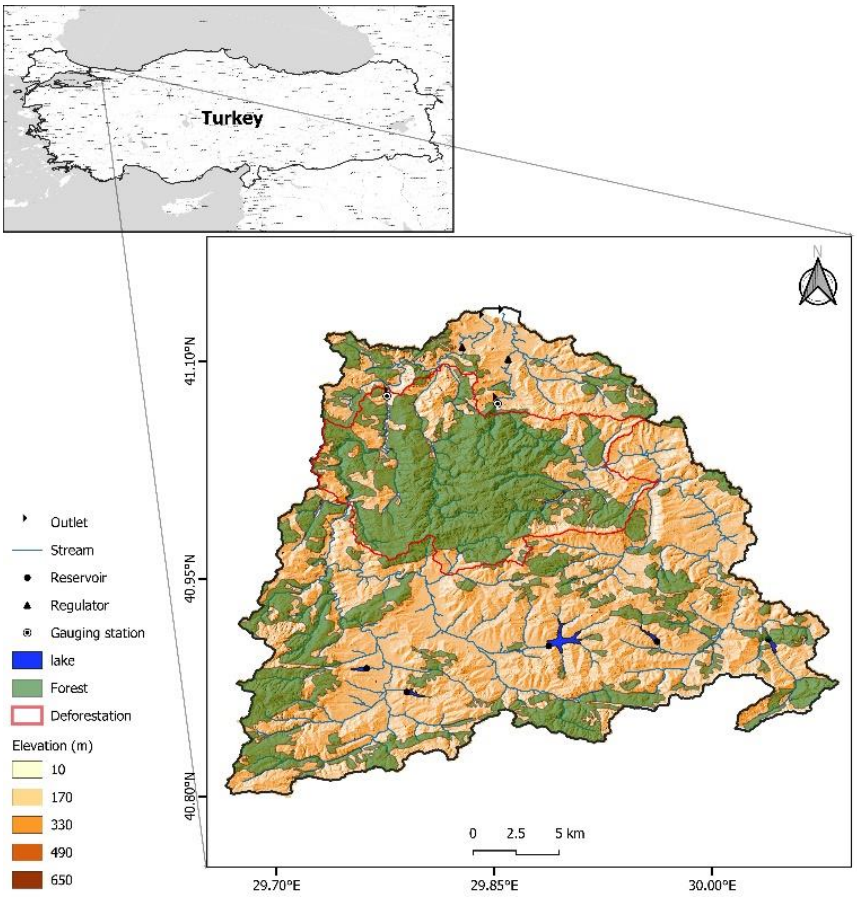

Figure 1. The location map of the study area, Göksu-Çanakdere rivers' watershed

Table 1. Description of scenarios used in this study. The mean degraded area is relative to the total watershed area (%)

Scenarios	Forest Patches Condition	Land-use Change (Forest Fires) (%)	Degraded Forest Area (ha)	Mean Degraded Area to Total Watershed Area (%)
Baseline	No land-use change	-	-	-
Scenario 1	Pastures + woodland + Mixed forest	25	2900	3.5
Scenario 2	Mixed forest + Broad leaved forest	50	5800	7
Scenario 3	Broad leaved forest	100	11000	14

Model performance evaluation

The model evaluation was performed based on the calibration and validation with a comparison of the measured and simulated discharge and sediment loads to constrain the model and achieve more robust characterizations of the land and the stream phases over the time step. The coefficient of determination (R2) and the Nash–Sutcliffe efficiency coefficient (NSE) (Nash and Sutcliffe, 1970) are two objective functions based on error statistics that were used as statistical and graphical model evaluation techniques to assess the model performance (Moriasi et al., 2007). The values of R^2 and NSE are determined by Equations 3 and 4, respectively.

$$R^2 = \frac{[\sum_i (Q_{m,i} - \bar{Q}_m)(Q_{s,i} - \bar{Q}_s)]^2}{\sum_i (Q_{m,i} - \bar{Q}_m)^2 \sum_i (Q_{s,i} - \bar{Q}_s)^2} \quad (3)$$

$$NSE = 1 - \frac{\sum_i (Q_m - Q_s)^2}{\sum_i (Q_{m,i} - \bar{Q}_m)^2} \quad (4)$$

where Q is a variable (for example, discharge), m and s represent observed or simulated, and i is the i^{th} observed or simulated data.

Table 2. Land use/cover distribution of the study area based on CORINE land cover classes classification and the converted land cover classes for the corresponding SWAT land cover codes with the coverage area and percentage of the watershed.

CORINE	SWAT	Land-use	Area coverage	
ID	Code	Definition	(ha)	(%)
112	URMD	Discrete urban fabric	178.8	0.23
121	UIDU	Industrial units	62.2	0.08
131	UMES	Mining sites	65.2	0.08
133	URCS	Construction sites	266.5	0.34
211	AGRL	Rain-fed arable land	26130.5	33.1
212	CRIR	Permanent irrigated land	477.7	0.60
222	ORCD	Fruit trees and berry gardens	1763	2.23
231	PAST	Pastures	69.5	0.09
242	CRGR	Mixed agriculture patterns	961.1	1.22
243	CRDY	Agricultural land	16686	21.1
311	FODB	Deciduous forest	27975.6	35.4
312	FRSD	Evergreen forest	118.7	0.15
313	FRST	Mixed forest	1128.8	1.43
321	GRAS	Grasslands	277.2	0.35
324	TUWO	Conditional woodland-shrub	2604.8	3.30
512	WATR	Water areas	200.2	0.25

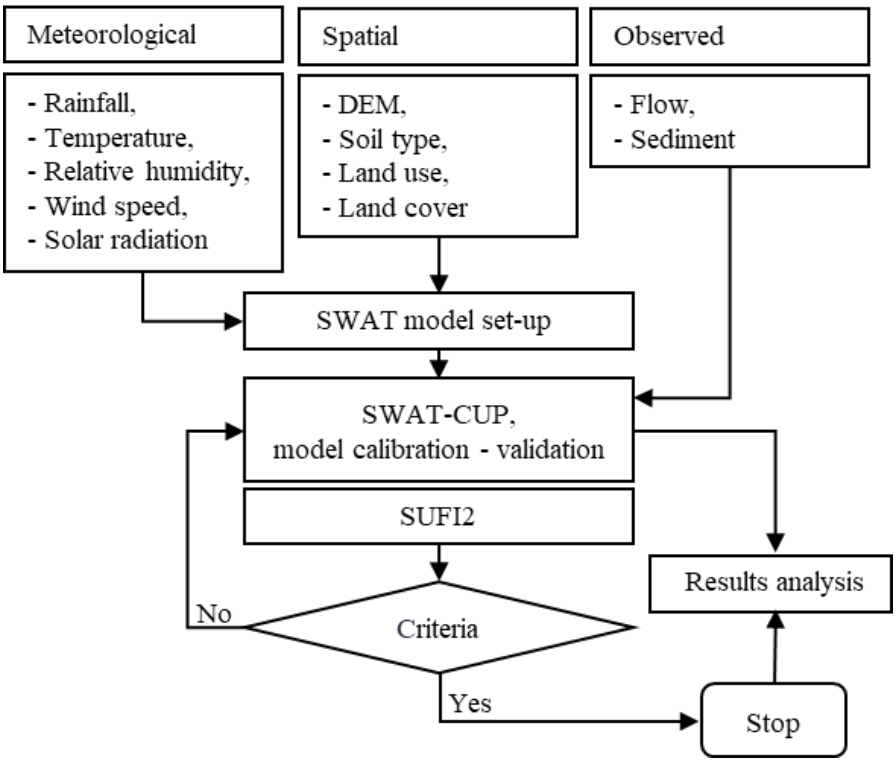

Figure 2. Flowchart of the fitting process

Results and discussion

Hydrological and sediment yield assessment

In this study, for water balance modeling and the ability to perform a combined calibration-uncertainty analysis, the Sequence Uncertainty Fitting - version 2 (SUFI-2) algorithm (Abbaspour et al., 2007) is used for the model calibration. The parameter uncertainty in the SUFI-2 algorithm is calculated based on the uncertainty of the entire input and output sources, such as the uncertainty of input precipitation data, land-use, soil types, and measured data. The simulation uncertainty is quantified by the 95 Percent Prediction Uncertainty (95 PPU) and the P-factor. 95PPU is calculated at the 2.5% (Lower 95PPU) and 97.5% (Upper 95PPU) levels of the cumulative distribution function of the output variable obtained from the Latin hypercube sampling method, disallowing 5% of the very bad simulations. The relative width of the 95% probability band is the R-factor. Auto calibration and validation and uncertainty analysis of the model was performed monthly using the SUFI-2 method within SWAT-CUP software (SWAT Calibration and Uncertainty Procedures) (Abbaspour et al., 2000). Thirteen relative sensitivity value parameters were evaluated and determined during the parameter estimation process in this study. The hydrological and sediment models were calibrated and validated using observational data from two rainfall stations for 2005 to 2013 and 2014 to 2017. Two years of data are used as the warm-up period for the model calibration. Sensitivity analysis results indicated that the most sensitive hydrological and sediment parameters were the SCS runoff curve number (CN2) and channel erodibility factor (CH_COV1), respectively. For the hydrological model, the second group of parameters with similar significance was the base flow alpha-factor (ALPHA_BF), the groundwater delay (GW_DELAY), and the threshold water depth in the shallow aquifer (GWQMN). For the sediment model, the exponent parameter for calculating the channel sediment routing (SPEXP), the average slope length (SLSUBBSN), the linear parameter for calculating the channel sediment routing (SPCON), the soil erodibility factor in USLE (USLE_K), and the USLE support practice factor (USLE_P) were the following sensitive parameters.

This study uses R^2 and NSE as objective functions to assess the model predictions and performance. The NSE values for discharge and sediment were obtained as 0.85 and 0.63 for calibration and 0.94 and 0.42 for validation periods, respectively. Model predictions of discharge and sediment loads were also evaluated in terms of coefficient of determination (R^2 = 0.86 and R^2 = 0.65) for calibration periods, respectively. Although the flow model performed well, the consistency between the observed and simulated sediment loads during the validation period was not satisfactory (NSE <0.5). However, for the validation period, higher performance values of the flow model (R^2 = 0.94) and good sediment model performance (R^2 = 0.58) were obtained, which indicates that the estimation of the research process is favored.

The linear regression analysis was performed to assess the relationship between monthly measured flow and suspended sediment for the 2005-to-2017-time steps (Figure 3). The result shows the high correlation between the measured monthly flow and the suspended sediment with a coefficient of determination of 0.85.

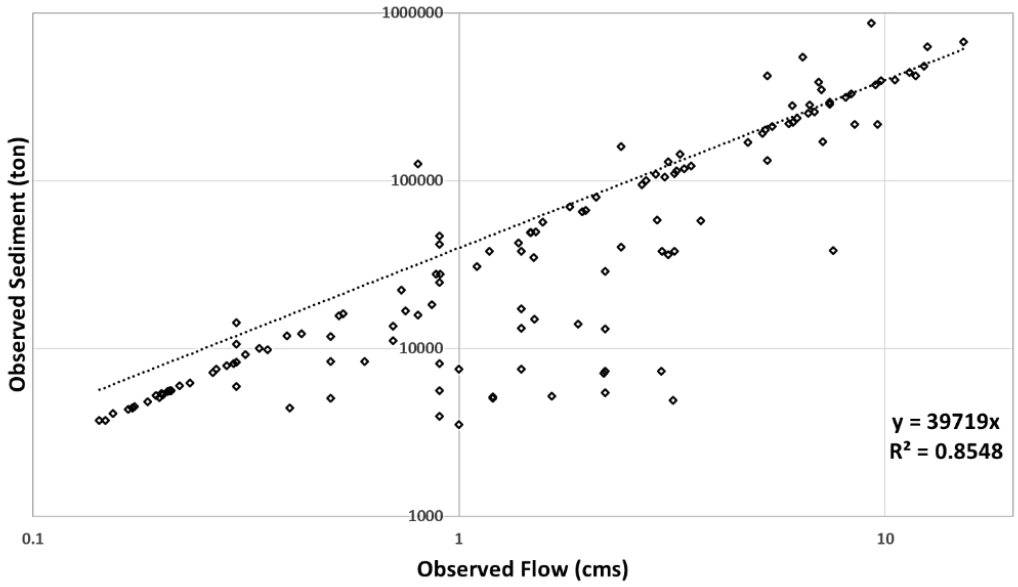

Figure 3. The relationship between monthly measured flow and suspended sediment (2005-2017)

Deforestation impacts on discharge and sediment yield

According to the scenarios under consideration, the resulting forest burnt areas and converting these areas to farmland is approaching between 3500 and 11000 hectares, corresponding to the model execution from the minor deforestation (scenario 1) to the massive deforestation (scenario 3), respectively. According to the designed scenarios, the average percentage of deforestation following forest fires is 8%, and the maximum amount is up to 14% of watershed's total area. The effects of deforestation due to the forest fires and changing land-use type for agricultural activities and its impact on discharge and sediment was evaluated by modifying the model land-use type of the input data. To this end, forest patches (i.e., the FODB land-use type in the SWAT code, as shown in Table 2) and lands overlapped by considered area for deforestation and its spatial distribution have been changed for the non-irrigated arable land (i.e., the AGRL land-use type in the SWAT code) for each scenario (scenarios 1 to 3). These changes are introduced into the SWAT database to generate new land-use categories. Finally, the model was re-run for each scenario using the new inputs and parameters to assess discharge and sediments yield. The model results of all scenarios for the water balance components are summarized according to the annual time step, as shown in Table 3.

In each SWAT simulation, different output files are generated, such as the HRU output file (output.hru), the sub-basin output file (output.sub), and the main channel or reach section output file (output.rch). Table 4 provides a brief description of the output variables demonstrated in the output summary files in Table 3. The output summary files from the HRU's, subbasins, and streams have provided averaged amounts over the entire simulation period for deforestation scenarios of selected sub-watershed in the study area. The model output shows that in the range of variations in the values of different scenarios, in comparing with the baseline scenario, the average annual total water yield (i.e., the total amount of surface runoff, lateral flow, and baseflow) of the deforestation sub-watershed increased by 3 to 10%. Succeeding the increase in water yield, and due to the high erosiveness ability of excessive surface runoff, and land preparation operations for agriculture such as plowing, disc harrowing, rake and slope leveling or wedding, thus the sediment yield after the forest fires and changing into the farmland has a significant increase of 3.5 times in compared with the sediment yield before the land-use change. After a significant increase in sediment yield, organic nitrogen and phosphorus were two components that increased remarkably, especially in Scenario 3, where they were 2-fold and 2.5-fold higher, respectively, than the baseline scenario (no change in land-use).

Increases in organic nitrogen and phosphorus may result from the imbalance on their inputs and outputs' cycle. In addition, land use conversion (deforestation) to cropland leads to accumulation and increase of nitrogen and phosphorus sources from litter decomposition and soil mineralization. (Aber, 1992; Watson et al., 2000). In contrast, the actual evapotranspiration and leaf area index decreased by 5% and 24%, respectively, in selected sub-basins due to deforestation and the removal of trees and vegetation from the ground. Correspondingly, the total transported nitrogen, phosphorus, and sediment into the reach indicate a significant increase in the post-deforestation scenario. The amount of dissolved oxygen transported out of reach during the time step showed the inverse ratio and decreased 11 to 17% after deforestation compared to the baseline scenario.

In addition to the quantitative statistics (Table 3), Figures 4 and 5 also provide an intuitive comparison of the graphical representations and the spatial distribution of the total annual amounts of surface runoff and amount of water (water yield) and sediment (sediment yield) that leaves the sub-basins and contributes to streamflow in the reach before (baseline) and post-deforestation (scenarios 1 to 3) scenarios within the time step for the selected subbasins in the study area. The average annual

streamflow from each sub-basin and the amounts of sediment transported with water into the reach during the time step is also superimposed on the spatial distribution map of water and sediment yield, as shown in Figure 4 and Figure 5, respectively. Each sub-basin has a unique number assigned to it during the watershed delineation phase of the model.

Table 3. Based on the model output of deforestation scenarios, a summary of the water balance components in yearly time steps. Model outputs were obtained from scenarios and average hydrologic response to deforestation during the simulation period of 13 years (2005 to 2017).

Outputs	Variables	Baseline	Scenario 1	Scenario 2	Scenario 3	Variations (%)
HRU	SYLD	758	863	896	1135	14-50
	SEDP	44	46	47	54	4-23
	USLE	1163	1247	1299	1557	7-34
	ORGN	237	260	264	311	10-31
	ORGP	40	46	47	56	13-39
	LAI[b]	123	120	119	93	24-2
SUB	WYLD	3897	4003	4074	4265	3-10
	SURQ	1877	1997	2082	2325	6-24
	SYLD	381	741	949	1702	95-347
	SEDP	28	39	46	70	40-153
	ORGN	159	239	292	458	50-188
	ORGP	26	44	56	91	70-254
	ET[b]	6502	6421	6351	6167	5-1
RCH[a]	SED_IN	0.51	1.13	1.38	2.25	121-341
	TOT_N	2.6	2.66	2.79	3.28	2-26
	TOT_P	0.87	0.89	0.94	1.1	2-27
	DISOX[b]	1.02	0.9	0.87	0.85	17-11

[a] All values in baseline and scenarios are multiplied by 10^6, [b] There is an inverse ratio.
***** The values in the table are presented for the selected sub-watershed of the study area.

Table 4. A brief description of the output variables that have been demonstrated in the output summary files (Arnold, 2012)

Outputs	Variable name	Definition
HRU	SYLD	Sediment yield (metric tons/ha)
	SEDP	Mineral phosphorus absorbed to sediment (kg P/ha)
	USLE	Soil loss calculated with the USLE* equation (metric tons/ha)
	ORGN	Transported amount of the organic nitrogen out of the HRU and into the reach (kg N/ha)
	ORGP	Transported amount of the organic phosphorus with sediment into the reach (kg P/ha)
	LAI	Leaf area index at the end of the time step
SUB	WYLD	Water yield, the total net amount of water that exit the sub-basin (mm H2O)
	SURQ	Surface runoff contribution to streamflow during the period (mm H2O)
	SYLD	Sediment yield (metric tons/ha) from the subbasin
	SEDP	Mineral phosphorus attached to sediment (kg P/ha)
	ORGN	Transported amount of the organic nitrogen out of the sub-basin and into the reach (kg N/ha)
	ORGP	Organic phosphorus transported with sediment into the reach (kg P/ha)
	ET	Sub-basin actual evapotranspiration during the time step (mm)
RCH	SED_IN	Transported sediment with water into reach during the period (metric tons)
	TOT_N	Total surface runoff nitrogen (kg)
	TOT_P	Total surface runoff phosphorus (kg)
	DISOX_IN	Transported dissolved oxygen into reach during the period (kg O2)

*Universal Soil Loss Equation

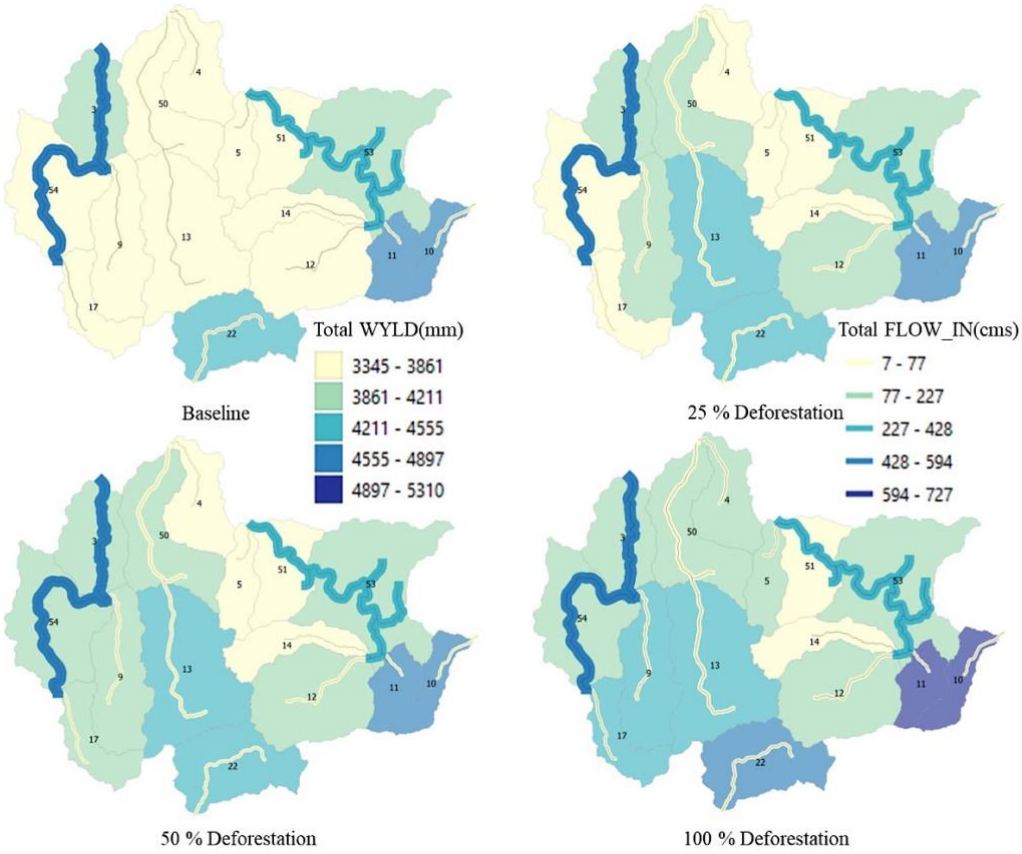

Figure 4. The total annual amounts of water yield for baseline and post-deforestation (scenarios 1 to 3) scenarios at the sub-catchment scale in time step (2005-2017)

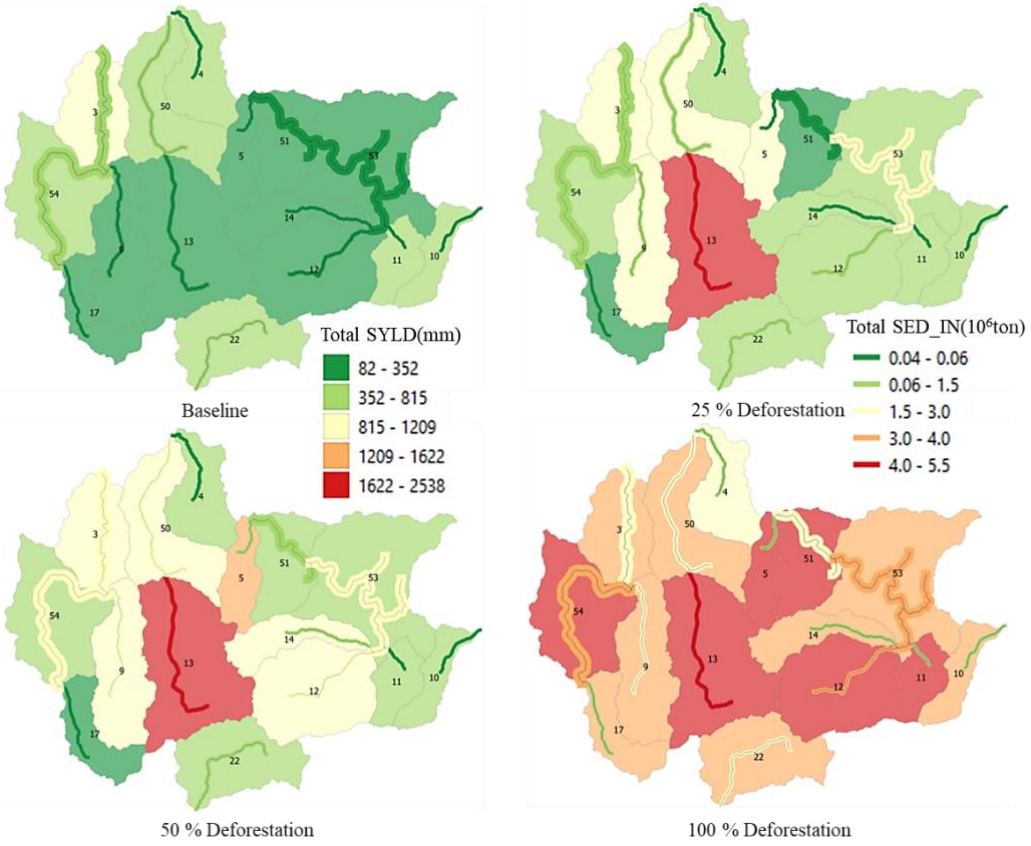

Figure 5. The total annual amounts of sediment yield for baseline and post-deforestation (from 1 to 3) scenarios at the sub-catchment scale in time step (2005-2017)

The progressive increase of deforestation area brings along a gradual increase in the annual mean flow rates, and the maximum runoff occurred in scenario 3 with the highest spatial distribution of deforestation where the surface runoff increased by 24% in compared with the baseline scenario and has raised from about 144 mm to 179 mm. In consequence of the degradation of forest and conversion, it into the farmland, a high contribution of the surface runoff to the streamflow and a significant increase in the amount of sediment transported into the stream has been observed that indicates a large amount of soil loss has occurred during the simulation time step. The amount of sediment eroded from HRUs and transported to the hydrological network of the selected sub-basins varied between 64.3- and 87.3-ton ha-1. Post-deforestation conditions resulted in an almost 50% increase compared with the baseline scenario, corresponding to an erosion rate increase of 29-ton ha^{-1}. Accordingly, soil loss from HRUs calculated with the USLE equation between the baseline and the scenario with the highest distribution of deforestation (scenario 3) changed from 89.5 to 119.8 (ton) and increased by 34% for the time step.

Erosion rates and sediment yield analysis identify areas with very high soil losses and their spatial distribution. The highest sedimentation rates were estimated particularly at sub-basins 5, 11-13, 51, and 54 of the selected area. Different parameters such as soil type and land topography (land on steep slopes) in the area can affect the erosion process and soil loss and cause to increase in soil erosion rate and sediment loss under high runoff conditions. According to the post-deforestation scenario analysis, the sedimentation rate of almost all distribution areas is very high, and the erosion rates would be above the tolerable soil losses limit (Verheijen et al., 2009). This result indicates that the selected sub-watershed has different areas where soil erosion is a substantial issue, and land degradation would be possibly higher than the soil formation rates in the watershed.

Model predictions and outputs indicate that after changes in land use/land cover due to deforestation, there is a high possibility of soil loss, sedimentation, and an increase in surface runoff. The hydrological and sediment model's outputs suggest that there are problems in landscape susceptibility to erosion and soil loss, and it is necessary to identify areas in the watershed that are at greater risk of erosion when land use/cover changes occur. Hence, the method used in this study can be helpful for decision-makers and an efficient approach to apply for the protection of forests from intensive impacts such as forest fires or deforestation.

Conclusion

Assessing the impact of land use/cover changes and deforestation on the hydrological response of watersheds is a critical step in reducing the likelihood of excessive surface runoff and erosion rates after deforestation. The development of hydrological models can effectively help management practices deal with the adverse effects of deforestation, such as soil erosion and sedimentation. This study investigated the applicability of the SWAT rainfall-runoff model to assess the hydrological consequences of land use/cover changes (i.e., deforestation) and their effects on surface runoff, erosion, and sediment load under baseline and post-deforestation scenarios. The results showed that the hydrological budget of the selected sub-basins has changed significantly in the post-deforestation period. In the deforestation scenario with the highest spatial distribution, due to the high erosivity (24% increase) of excessive surface runoff after deforestation, sediment yield increased 3.5 times. This study recommends the potential use of hydrological and erosion models to analyze the impact of deforestation on sediment load under different scenarios. The consequences of deforestation on hydrological services can help decision-makers choose better post-deforestation mitigation plans to limit the impact of the forest degradation on the sediment load as well as its environmental issues.

Compliance with Ethical Standards

Conflict of interest

The authors declared no actual potential or perceived conflict of interest for this research article.

Author contribution

The contribution of the authors to the present study is equal. All the authors read and approved the final manuscript. All the authors verify that the Text, Figures, and Tables are original and have not been published before.

Ethical approval

Ethics committee approval is not required.

Funding

No financial support was received for this study.

Data availability

Not applicable.

Consent for publication

Not applicable.

Acknowledgments

The study was supported by the Scientific Research Projects Coordination Unit of Istanbul University-Cerrahpasa, Project number FDK-2018-29656. The authors would like to thank the Scientific Research Projects Coordination Unit of Istanbul University-Cerrahpasa for their support. This study is part of the first author's Ph.D. thesis.

References

Abbaspour, K. C., Vejdani, M, and Haghighat, S. (2000). SWAT-CUP Calibration and Uncertainty Programs for SWAT. Transactions of the American Society of Agricultural Engineers, 43(5), 1596–1602. Doi: https://doi.org/10.13031/2013.3000

Abbaspour, K. C., Yang, J., Maximov, I., Siber, R., Bogner, K., Mieleitner, J., Zobrist, J., and Srinivasan, R. (2007). Modelling hydrology and water quality in the pre-alpine/alpine Thur watershed using SWAT. Journal of Hydrology, 333(2–4), 413–430. Doi: https://doi.org/10.1016/j.jhydrol.2006.09.014

Aber, J. D. (1992). Nitrogen cycling and nitrogen saturation in temperate forest ecosystems. Trends in Ecology and

Evolution, 7(7), 220–224. Doi: https://doi.org/10.1016/0169-5347(92)90048-G
Aksoy, E., Panagos, P., Montanarella, L., and Jones, A. (2010). Integration of the Soil Database of Turkey. In Earth. Doi: http://dx.doi.org/10.2788/77892
Aliye, A., Modibbo, N., Medugu, N., and Ayo, O. (2014). Impacts of Deforestation on Socio-Economic Development of Akwanga Nasarawa State. International Journal of Science, Environment and Technology, 3(2), 403–416.
Amundson, R., Berhe, A., Hopmans, J., Olson, C., Sztein, A. E., and Sparks, D. (2015). Soil and human security in the 21st century. Science, 348(6235). Doi: https://doi.org/10.1126/science.1261071
Arnold, J., Allen, P., and Bernhardt, G. (1993). A comprehensive surface-groundwater flow model. Journal of Hydrology, 142(1–4), 47–69. Doi: https://doi.org/10.1016/0022-1694(93)90004-S
Arnold, J. G., Moriasi, D. N., Gassman, P. W., Abbaspour, K. C., White, M. J., Srinivasan, R., Santhi, C., Harmel, R. D., and Griensven, A. Van. (2012). Swat: Model Use, Calibration, and Validation. 55(4), 1491–1508. Doi: http://dx.doi.org/10.13031/2013.42256
Atalay, I. (1986). Vegetation formations of Turkey. Travaux - Institut de Geographie de Reims, 65–66, 17–30. Doi: https://doi.org/10.3406/tigr.1986.1183
Avwunudiogba, A., and Hudson, P. F. (2014). A Review of Soil Erosion Models with Special Reference to the needs of Humid Tropical Mountainous Environments. European Journal of Sustainable Development, 3(4), 299–310. Doi: https://doi.org/10.14207/ejsd.2014.v3n4p299
Bettess, R., Fisher, K., Hardwick, M., Holmes, N., Mant, J., Sayers, P., Sear, D., and Thorne, C. (2011). Key Recommendations for Channel management (Issue Phase 2). Environment Agency, Bristol, UK.
Bonan, G. B. (1999). Frost Followed the Plow: Impacts of Deforestation on the Climate of the United States. Ecological Applications, 9(4), 1305. Doi: https://doi.org/10.2307/2641398
Bredemeier, M. (2010). Forest, climate and water issues in Europe. Ecohydrology, 130(February), 126–130.
Brevik, E. C. (2006). Soil health and productivity. Soils, Plant Growth Crop Prod. Encyclopedia of Life Support Systems (EOLSS), I. Retrieved from https://www.eolss.net/sample-chapters/c10/E1-05A-04-00.pdf
Chrisphine, O., Maryanne, O., and Boitt, K. M. (2015). Assessment of Hydrological Impacts of Mau Forest, Kenya. Journal of Waste Water Treatment & Analysis, 07(01), 1–7. Doi: https://doi.org/10.4172/2157-7587.1000223
Citiroglu, H., Barut, I., and Zuran, A. (2011). Groundwater vulnerability assessment in the Loussi polje area, N Peloponessus: the PRESK method. In Advances in the Research of Aquatic Environment. Doi: https://doi.org/10.1007/978-3-642-24076-8_39
CLC. (2018). European Union, Copernicus Land Monitoring Service 2018, European Environment Agency (EEA), 1, 129. Retrieved from https://land.copernicus.eu/
Collins, A. L., and McGonigle, D. F. (2008). Monitoring and modelling diffuse pollution from agriculture for policy support: UK and European experience. Environmental Science and Policy, 11(2), 97–101. Doi: https://doi.org/10.1016/j.envsci.2008.01.001
Cullu, M. A., Gunal, H., Akca, E., and Kapur, S. (2018). Soil Geography. In Encyclopedia of Environmental Change (pp. 105–109). The Soils of Turkey. World Soils Book Series. Springer, Cham. Doi: https://doi.org/10.4135/9781446247501.n3605
De Vente, J., Poesen, J., Verstraeten, G., Govers, G., Vanmaercke, M., Van Rompaey, A., Arabkhedri, M., and Boix-Fayos, C. (2013). Predicting soil erosion and sediment yield at regional scales: Where do we stand? Earth-Science Reviews, 127, 16–29. Doi: https://doi.org/10.1016/j.earscirev.2013.08.014
Farley, K., Jobbágy, E., and Jackson, R. (2005). Effects of afforestation on water yield: A global synthesis with implications for policy. Global Change Biology, 11(10), 1565–1576. Doi: https://doi.org/10.1111/j.1365-2486.2005.01011.x
Gellis, A., Fitzpatrick, F., and Schubauer-Berigan, J. (2016). A Manual to Identify Sources of Fluvial Sediment. U.S. Environmental Protection Agency, Washington, DC, EPA/600/R1(September), 106. Retrieved from https://nepis.epa.gov/Exe/ZyPDF.cgi/P100QVM1.PDF?Dockey=P100QVM1.PDF
Hargreaves, G. H., and Samani, Z. A. (1985). Reference Crop Evapotranspiration From Ambient Air Temperature. Applied Engineering in Agriculture. 1(2): 96-99. Doi: http://dx.doi.org/10.13031/2013.26773
Hassan, M. A., Roberge, L., Church, M., More, M., Donner, S. D., Leach, J., and Ali, K. F. (2017). What are the contemporary sources of sediment in the Mississippi River? Geophysical Research Letters, 44(17), 8919–8924. Doi: https://doi.org/10.1002/2017GL074046
Hughes, R., Kauffman, J., and Jarmaillo, V. (2000). Ecosystem-Scale Impacts of Deforestation and Land Use in a Humid Tropical Region of Mexico. Ecological Applications, 10(2), 515. Doi: https://doi.org/10.2307/2641111
Iwata, T., Nakano, S., and Inoue, M. (2003). Impacts of past riparian deforestation on stream communities in a tropical rain forest in Borneo. Ecological Applications, 13(2), 461–473. Doi: https://doi.org/10.1890/1051-0761(2003)013[0461:IOPRDO]2.0.CO;2
Izquierdo, A. E., and Grau, H. R. (2009). Agriculture adjustment, land-use transition and protected areas in Northwestern Argentina. Journal of Environmental Management, 90(2), 858–865. Doi: https://doi.org/10.1016/j.jenvman.2008.02.013
Jenkins, A. P., Jupiter, S. D., Qauqau, I., and Atherton, J. (2007). The importance of ecosystem-based management for conserving aquatic migratory pathways on tropical high islands: a case study from Fiji. Aquatic Conservation: Marine and Freshwater Ecosystems, 656(October 2006), 636–656.
Juárez-Orozco, S., Siebe, C., and Fernández, D. (2017). Causes and Effects of Forest Fires in Tropical Rainforests: A Bibliometric Approach. Tropical Conservation Science, 10. Doi: https://doi.org/10.1177/1940082917737207

Kük, M., and Burgess, P. (2010). The Pressures on, and the Responses to, the State of Soil and Water Resources of Turkey. Ankara Üniversitesi Çevrebilimleri Dergisi, March, 199–211. Doi: https://doi.org/10.1501/csaum_0000000036

Langdale, G. W., West, L. T., Bruce, R. R., Miller, W. P., & Thomas, A. W. (1992). Restoration of eroded soil with conservation tillage. Soil Technology, 5(1), 81–90. Doi: https://doi.org/10.1016/0933-3630(92)90009-P

Li, Y., Zhao, M., Mildrexler, D. J., Motesharrei, S., Mu, Q., Kalnay, E., Zhao, F., Li, S., and Wang, K. (2016). Potential and actual impacts of deforestation and afforestation on land surface temperature. Journal of Geophysical Research, 121(24), 14372–14386. Doi: https://doi.org/10.1002/2016JD024969

Maxwell, S. L., Fuller, R. A., Brooks, T. M., and Watson, J. E. M. (2016). Biodiversity: The ravages of guns, nets and bulldozers. Nature, 536(7615), 143–145. Doi: https://doi.org/10.1038/536143a

Monteith, J. L. (1965). Evaporation and Environment. Symposia of the Society for Experimental Biology., 19, 205–234. Retrieved from https://repository.rothamsted.ac.uk/item/8v5v7

Moriasi, D. N., Arnold, J. G., M. W. Van Liew, R. L. Bingner, Harmel, R. D., and T. L. Veith. (2007). Model Evaluation Guidelines for Systematic Quantification of Accuracy in Watershed Simulations. American Society of Agricultural and Biological Engineers, 50(3), 885–900. Retrieved from https://swat.tamu.edu/media/1312/moriasimodeleval.pdf

Nash, J. E., and Sutcliffe, J. V. (1970). River flow forecasting through conceptual models part I — A discussion of principles. Journal of Hydrology, 10(3), 282–290. Doi: https://ui.adsabs.harvard.edu/link_gateway/1970JHyd...10..282N/doi:10.1016/0022-1694(70)90255-6

Neitsch, S., Arnold, J., Kiniry, J., and Williams, J. (2011). Soil & Water Assessment Tool Theoretical Documentation Version 2009. Texas Water Resources Institute, 1–647. Doi: https://doi.org/10.1016/j.scitotenv.2015.11.063

Neitsch, S. L., Arnold, J. G., Kiniry, J. R., and Williams., J. R. (2005). Soil and Water Assessment Tool User's Manual Version 2005. Diffuse Pollution Conference Dublin, 494. Retrieved from http://swat.tamu.edu/media/1292/swat2005theory.pdf

Owens, P. N., Batalla, R. J., Collins, A. J., Gomez, B., Hicks, D. M., Horowitz, A. J., Kondolf, G. M., Marden, M., Page, M. J., Peacock, D. H., Petticrew, E. L., Salomons, W., & Trustrum, N. A. (2005). Fine-grained sediment in river systems: Environmental significance and management issues. River Research and Applications, 21(7), 693–717. Doi: https://doi.org/10.1002/rra.878

Pattanayak, S. K., and Wendland, K. J. (2007). Nature's care: Diarrhea, watershed protection, and biodiversity conservation in Flores, Indonesia. Biodiversity and Conservation, 16(10), 2801–2819. Doi: https://doi.org/10.1007/s10531-007-9215-1

Pimentel, D., and Burgess, M. (2013). Soil erosion threatens food production. Agriculture (Switzerland), 3(3), 443–463. Doi: https://doi.org/10.3390/agriculture3030443

Pimentel, D., Harvey, C., Resosudarmo, P., Sinclair, K., Kurz, D., McNair, M., Crist, S., Shpritz, L., Fitton, L., Saffouri, R., and Blair, R. (1995). Environmental and economic costs of soil erosion and conservation benefits. Science, 267(5201), 1117–1123. Doi: https://doi.org/10.1126/science.267.5201.1117

Priestley, C. H. B., and Taylor, R. J. (1972). On the Assessment of Surface Heat Flux and Evaporation Using Large-Scale Parameters. Monthly Weather Review, 100(2), 81–92.

Ritter, J. (2012). Wind Erosion - Causes and Effects. ProEnvironment/ProMediu, 12(38), 1–8. Retrieved from http://www.omafra.gov.on.ca/english/engineer/facts/12-053.htm

Rocha-Santos, L., Pessoa, M. S., Cassano, C. R., Talora, D. C., Orihuela, R. L. L., Mariano-Neto, E., Morante-Filho, J. C., Faria, D., & Cazetta, E. (2016). The shrinkage of a forest: Landscape-scale deforestation leading to overall changes in local forest structure. Biological Conservation, 196, 1–9. Doi: https://doi.org/10.1016/j.biocon.2016.01.028

Schüler, G. (2006). Identification of flood-generating forest areas and forestry measures for water retention. Forest Snow and Landscape Research, 80(1), 99–114. Retrieved from https://www.dora.lib4ri.ch/wsl/islandora/object/wsl%3A15461

Symes, W. S., Edwards, D. P., Miettinen, J., Rheindt, F. E., and Carrasco, L. R. (2018). Combined impacts of deforestation and wildlife trade on tropical biodiversity are severely underestimated. Nature Communications, 9(1). Doi: https://doi.org/10.1038/s41467-018-06579-2

USDA. (1972). USDA Soil Conservation Service. National Engineering Handbook Section 4 Hydrology, August, Chapters 4-10. Retrieved from https://directives.sc.egov.usda.gov/OpenNonWebContent.aspx?content=18389.wba

Verheijen, F. G. A., Jones, R. J. A., Rickson, R. J., and Smith, C. J. (2009). Tolerable versus actual soil erosion rates in Europe. Earth-Science Reviews, 94(1–4), 23–38. Doi: https://doi.org/10.1016/j.earscirev.2009.02.003

Wardle, D. A., Bardgett, R. D., Klironomos, J. N., Setälä, H., Van Der Putten, W. H., and Wall, D. H. (2004). Ecological linkages between aboveground and belowground biota. Science, 304(5677), 1629–1633. Doi: https://doi.org/10.1126/science.1094875

Watson, R., Noble, R., Bolin, B., Ravindranath, N., Verardo, D., and Dokken, D. (2000). Land Use, Land-Use Change and Forestry (p. 20pp). Retrieved from https://archive.ipcc.ch/ipccreports/sres/land_use/index.php?idp=0

Wenger, A. S., Atkinson, S., Santini, T., Falinski, K., Hutley, N., Albert, S., Horning, N., Watson, J. E. M., Mumby, P. J., and Jupiter, S. D. (2018). Predicting the impact of logging activities on soil erosion and water quality in steep, forested tropical islands. Environmental Research Letters, 13(4). Doi: https://doi.org/10.1088/1748-9326/aab9eb

Wilk, J., Andersson, L., and Plermkamon, V. (2001). Hydrological impacts of forest conversion to agriculture in a large river basin in Northeast Thailand. Hydrological Processes, 15(14), 2729–2748. Doi: https://doi.org/10.1002/hyp.229

Williams, J., Karl G., and Bruce P. V. H. (1975). Use of the Modified Universal Soil Loss Equation for average annual sediment yield estimates on small rangeland drainage basins. Present and Prospective Technology for Predicting Sediment Yield and Sources. U.S. Dept. Agrie., pp 244-252. Retrieved from https://iahs.info/uploads/dms/6694.413-422-159-Jackson.pdf

WWF. (2017). Causes and effects of global forest fires. Retrieved from https://www.wwf.de/fileadmin/fm-wwf/Publikationen-PDF/WWF-Study-Forests-Ablaze.pdf

Yen, H., Ahmadi, M., White, M. J., Wang, X., and Arnold, J. G. (2014). C-SWAT: The Soil and Water Assessment Tool with consolidated input files in alleviating computational burden of recursive simulations. Computers and Geosciences, 72, 221–232. Doi: https://doi.org/10.1016/j.cageo.2014.07.017